Journal of
Composites Science

MDPI

Article

Nonisothermal Crystallization Kinetics of Polylactic Acid under the Influence of Polyolefin Elastomers

Azadeh Khosravi [1], Abdolhossein Fereidoon [1], Mohammad Mehdi Khorasani [2], Vincent Berthe [3], Henri Vahabi [4], Seyed Mohammad Reza Paran [5,*], Ghasem Naderi [5] and Mohammad Reza Saeb [6,*]

1 Department of Mechanical Engineering, Semnan University, Semnan 35131, Iran; azadeh_khosravi_82@yahoo.com (A.K.); afereidoon@semnan.ac.ir (A.F.)
2 Petrochemical Research and Technology Company (NPC-rt), National Petrochemical Company (NPC), Tehran P.O. Box 14358-84711, Iran; mehdi.khorasani@gmail.com
3 Department of Materials Research and Technology (MRT), Luxembourg Institute of Science and Technology (LIST), 5 Avenue des Hauts-Fourneaux, L-4362 Esch-sur-Alzette, Luxembourg; vincent.berthe@list.lu
4 Université de Lorraine, CentraleSupélec, LMOPS, F-57000 Metz, France; henri.vahabi@univ-lorraine.fr
5 Department of Polymer Processing, Iran Polymer and Petrochemical Institute, Tehran P.O. Box 14965/115, Iran; G.naderi@ippi.ac.ir
6 Department of Resin and Additives, Institute for Color Science and Technology, Tehran P.O. Box 16765-654, Iran
* Correspondence: m.paran@aippi.ac.ir (S.M.R.P.); saeb-mr@icrc.ac.ir (M.R.S.); Tel.: +98-912-4213-732 (S.M.R.P.); +98-912-8264-307 (M.R.S.); Fax: +98-2148-662-520 (S.M.R.P.)

Received: 15 April 2020; Accepted: 29 May 2020; Published: 2 June 2020



Abstract: Crystallization kinetics of various blends of poly(lactic acid) (PLA)/polyolefin elastomer (POE) was studied through nonisothermal experimental investigations and theoretical approaches. The PLA/POE blends were prepared in a melt mixing process by using two types of POEs and compatibilizers. The rubber phases used were adopted on the basis of polyethylene (PE) and polypropylene (PP) type olefin elastomers. The effects of two kinds of compatibilizers containing ethylene vinyl acetate copolymer (EVA) and ethylene acrylic ester-glycidyl methacrylate terpolymer (EGMA) on the morphology and various parameters of crystallization of PLA were investigated using scanning electron microscopy (SEM) and differential scanning calorimeter (DSC) measurements, respectively. The morphology investigations on PLA blends containing PP based olefin elastomers showed that the introduction of EGMA compatibilizer into the matrix led to a more than 100% reduction in the size of the rubber droplets. The experimental measurements of crystallization behavior of various PLA/POE blends showed that the POEs and compatibilizers could cause a fall in the initial crystallization temperature more than 13 °C. The theoretical approaches used for studying the kinetics of crystallization of PLA in the presence of various POEs and compatibilizers indicated a decrease in the crystallinity of PLA and a 64% reduction in the activation energy compared to the neat PLA. The results suggest that the largest variation in the crystallization kinetic parameters of PLA was resulted from the PP based olefin elastomer and EGMA compatibilizer.

Keywords: crystallization kinetics; poly(lactic acid) (PLA); polyolefin elastomer (POE); compatibilizer; morphology

1. Introduction

The mechanical behavior of polymers is greatly influenced by their thermal properties [1] and thermal histories [2], which can be determined experimentally [3]. The crystallinity is one of the most

important factors determining the ultimate physical and mechanical properties [4] of semi-crystalline polymers, especially above the glass–rubber transition temperature (Tg). The crystallization behavior of various semi-crystalline polymers such as polyethylene, polypropylene, and polyamides can be evaluated by differential scanning calorimetry (DSC) techniques via isothermal and nonisothermal procedures [5]. The study of the kinetics of the crystallization behavior of polymers under isothermal [6] or nonisothermal [7] conditions is the best way to understand the processability and the effect of various processing parameters such as the heating/cooling rates and the processing temperature on the crystallization mechanism. Crystallization kinetics can be studied through the simultaneous use of experimental and theoretical analyses.

Poly(lactic acid) (PLA) is a semi-crystalline polymer used in various industries, particularly in fabrication of biaxial oriented films [8], thermoforming products [9], and filaments for 3D printings [10]. However, PLA is a biodegradable polymer with properties and the performance highly sensitive to the processing conditions [11]. Therefore, the crystallization of PLA has been studied from various aspects to control its processability, ultimate mechanical properties, and thermal stability [12]. Kulinski et al. [13] investigated the effect of various grades of poly(ethylene glycol) on the crystallization behavior of PLA and reported a fall in the T_g and higher potential of PLA to cold crystallization. Yokohara et al. [14] evaluated the crystallization behavior of PLA containing poly(butylene succinate) (PBS) and found that the introduction of PBS into the PLA matrix increased the crystallization of PLA even though PBS was in the molten state. Pantani et al. [15] studied the isothermal crystallization kinetics of virgin and processed PLA under extrusion and injection molding methods. It was found that the kinetic constant of injection molded PLA was one order of magnitude faster than the extruded PLA and twice of the virgin PLA.

The brittleness of PLA [16] with its low impact strength [17] has led to major limitations in the use of this polymer in many engineering applications. The literature survey showed that extensive efforts have been recently made to tackle this problem. One of the most commonly used approaches was the blending of PLA with highly flexible polymers such as natural rubber [18], epoxidized natural rubber [19], linear low density polyethylene [20], and polyolefin elastomers [21]. However, the requirement of good interfacial interactions between the PLA and the second polymer phase is an essential factor to meet the required properties, such as high tensile strength, impact strength, and elongation at break [22,23]. Recently, PLA blends toughened with polyolefin elastomers have been the focus of researchers due to their cost benefits and good processability [24]. Wu et al. [25] reported on the effect of the olefin block copolymer on the toughness strength and mechanical properties of PLA in the presence of a compatibilizer and found that the elastomer phase could enhance the impact toughness of PLA up to 25 times compared to the neat PLA. However, the tensile strength of toughened PLA was unsurprisingly decreased by 87% with respect to the neat PLA. Jiang et al. [26] evaluated the effect of various rubber components on the toughness of PLA and reported that poly(ethylene-glycidyl methacrylate) was more efficient in comparison with maleic anhydride grafted poly(styrene-ethylene/butylene-styrene) triblock elastomer and poly(ethylene-co-octene) to give a PLA blend with improved impact toughness. Wu et al. [27] manipulated the morphology of PLA reinforced with olefin block copolymer through reactive melt blending using ethylene-glycidyl methacrylate (EGMA) as a compatibilizer. Their study showed that there was a chemical interaction between PLA and EGMA, while only physical interaction occurred between the olefin block copolymer (OBC) and EGMA, which led to an asymmetric dispersed phase morphology. Their results indicated that the crystallization behavior of PLA depends on both the content of the dispersed phase and the type of the second polymer used in the blend.

In previous reports [28] on the crystallization kinetics of multiphase polymeric systems based on theoretical models, we indicated that the key parameters in crystallization behavior such as the initial crystallization temperature, crystallization rate, and activation energy could be significantly varied by varying the dispersed phase content [28]. As indicated in the literature survey, the crystallization

of PLA could be deteriorated by various processing parameters and adsitives, where focusing on its crystallization kinetics would be a useful guide to develop PLA for engineering applications.

The methodology of this article includes the melt mixing of PLA with two grades of polyolefin elastomer (POE) (80/20 w/w) in the presence of external compatibilizer. The effects of two kinds of compatibilizers containing ethylene vinyl acetate copolymer (EVA) and ethylene acrylic ester-glycidyl methacrylate terpolymer (EGMA) on the various parameters of the crystallization of PLA were investigated using appropriate theoretical kinetic models. Furthermore, the effects of various compatibilizers on the morphology of the prepared PLA/POE blends were evaluated by scanning electron microscopy (SEM) and the size of the dispersed rubber phase was calculated using statistical analysis.

2. Theoretical Background

Mathematical methods provide a comprehensive evaluation of the nonisothermal crystallization kinetics of various polymeric systems. The degree of phase conversion, X_t, whci is a components of the Avrami equation [29] inisothermal mode can be expressed as follows:

$$X_t = 1 - e^{-Z_t t^n}, \tag{1}$$

where Z_t depends on the nucleation and the growth rate and n depends on the process dimensionalities and is held to have an integer value between 1 and 4, which states the nature of the transformation, the Avrami constant and Avrami exponent, respectively. These parameters can be determined from [28]:

$$\log[-\ln(1 - X_t)] = \log Z_t + n\log t, \tag{2}$$

By plotting the $\log[-\ln(1 - X_t)]$ vs. $\log t$, the parameters Z_t and n can be obtained. The half-time of crystallization, defined as the time to reach 50% of crystallization, can be defined as the following equation [30]:

$$t_{1/2} = (\ln 2/Z_t)^{1/n} \tag{3}$$

Crystallization rate constant of in nonisothermal crystallization os adefoned as:

$$\log Z_C = \frac{\log Z_t}{dT/dt}, \tag{4}$$

As the Avrami equation is based on the isothermal crystallization mode, Ozawa [7] changed it to the nonisothermal applicable model as the following relation:

$$1 - X_t = e^{-K(T)/\frac{dT}{dt}^m}, \tag{5}$$

$$\log[-\ln(1 - X_t)] = \log K(T) - m\log\left(\frac{dT}{dt}\right), \tag{6}$$

The plot of $\log[-\ln(1 - X_t)]$ vs. $\frac{dT}{dt}$ gives a straight line from which m is obtained, while $K(T)$ is obtained from the vertical intercept.

Mo et al. [30] presented an equation based on Avrami and Ozawa equations, which linked the cooling rate and time as:

$$\log\left(\frac{dT}{dt}\right) = \log F(T) - a\log t, \tag{7}$$

$$F(T) = \left[\frac{K(T)}{Z_t}\right]^{1/m}, \tag{8}$$

$$a = \frac{n}{m}, \tag{9}$$

where $F(T)$ is the velocity parameter determined from the vertical intercept of the best-fittedline drawn through the data points for each cooling rate at a given value of X_t (the log $(\frac{dT}{dt})$ as a function of log (t)). The parameter a could be achieved from the slope of the line of log $\left(\frac{dT}{dt}\right)$ as a function of log (t). It should be noted that the overall nonisothermal crystallization rate and activation energy resulting from the Avrami and Ozawa equations can not clearly reflect the crystallization behavior of the polymers. Kissinger et al. [31] presented the activation energy of the crystallization process by using the variation of the crystallization peak temperature with the cooling rate as the following equation:

$$\frac{d\left[\ln\left(\frac{\frac{dT}{dt}}{Tc_p^2}\right)\right]}{d\left(\frac{1}{Tc_p}\right)} = -\frac{\Delta E}{R}, \tag{10}$$

where T_p is the crystallization peak temperature and R is the universal gas constant.

3. Experimental

3.1. Materials

Poly(L-lactic acid) (PLA), Ö5 BIOKAS, with a melt flow index (MFI) of 7 g/10 min (210 °C, 2.16 kg), specific gravity of 1.24 g/cm^3 and melting point of 155–170 °C was obtained from Chemiekas GmbH, Austria. DF810 Tafmer is a specialty, ethylene based α-olefin elastomer (TPO) grade supplied by Mitsui Chemicals, Japan with a MFI of 1.2 g/10 min (190 °C, 2.16 kg), density of 0.885 g/cm^3, and softening temperature of 66 °C. Vistamaxx 6102 is primarily composed of isotactic propylene repeat units with random ethylene distribution purchased from ExxonMobil Chemicals, USA, with a MFI of 1.4 g/10 min (190 °C, 2.16 kg), density of 0.862 g/cm^3, and softening temperature of 52 °C. A random terpolymer of ethylene, methyl acrylate, and glycidyl methacrylate (EGMA) was used as the reactive precursor for the compatibilization of PLA, and POE was LOTADER® AX8900 from Arkema, France, which contains 24 wt% methyl acrylate, 8 wt% glycidyl methacrylate, a density of 0.94 g/cm^3, and MFI of 6 g/10 min (190 °C, 2.16 kg). Ethylene-vinyl acetate copolymer (EVA), VA600, purchased from Lotte Chemical Co., South Korea, was used as a compatibilizer to tie PLA with POE, which contained 19% vinyl acetate, had a density of 0.939 g/cm^3, and MFI of 2.5 g/10 min (190 °C, 2.16 kg).

3.2. Sample Preparation

The PLA/POE blends containing various compatibilizers, according to Table 1, were prepared through a direct melt mixing process in a laboratory size internal mixer (Brabender Plasti-Corder, W50, Duisburg, Germany) at 190 °C and 60 rpm for 5 min. The internal mixer had a chamber with a 55 mL mixing volume and fill factor of 0.8. grades of POEs, named PE and PP, are referred to as Tafmer and Vistamaxx, respectively. For a more accurate comparison, PLA granolas were once melted in accordance with the above conditions.

Table 1. The prepared poly(lactic acid) (PLA)/polyolefin elastomer (POE) formulations. EVA: ethylene vinyl acetate copolymer; EGMA: ethylene acrylic ester-glycidyl methacrylate terpolymer.

Sample Code	PLA (phr)	POE (phr)	EVA (phr)	EGMA (phr)
PLA	100	-	-	-
PLAPE	80	20	-	-
PLAPEVA	80	20	4	-
PLAPEGMA	80	20	-	4
PLAPP	80	20	-	-
PLAPPVA	80	20	4	-
PLAPPGMA	80	20	-	4

3.3. Characterization

The morphologies of various PLA/POE blends were imaged on a TESCAN VEGA3 (TESCAN, Brno, Czech) scanning electron microscopy (SEM). Gold sputtered cryogenically fracture surfaces of samples were seen an accelerated voltage of 20 kV. Three types of samples underwent microscopic analyses. Figure 1 shows the SEM micrographs of three samples without etching, with etching in xylene at room temperature for 20 h, and with etching in xylene at 70 °C for 6 h. It was concluded that etching at room temperature was as good as that at 70 °C, but because of safety issues, etching at room temperature was selected. Therefore, samples were etched in xylene at room temperature for 20 h for the extraction of the POE phase.

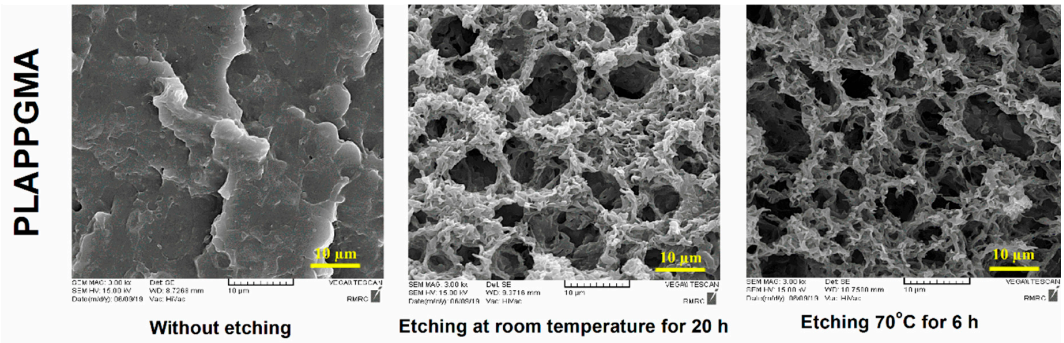


Figure 1. The comparison between different ways of sample etching in xylene.

The particle size of the POE phase was measured in representative zones of the cryogenically fractured specimens. The number (D_n) and volume (D_v) average diameters were determined using the following equations [32]:

$$D_n = \frac{\sum_{i=1}^{\infty} n_i D_i}{\sum_{i=1}^{\infty} n_i}, \tag{11}$$

$$D_v = \frac{\sum_{i=1}^{\infty} n_i D_i^4}{\sum_{i=1}^{\infty} n_i D_i^3}, \tag{12}$$

where D_i and n_i are the diameter and the number of counted particles, respectively.

The nonisothermal crystallization behavior of the PLA/POE blends was analyzed by means of Perklin Elmer 4000, USA differential scanning calorimeter (DSC). Before testing, all the samples were dried at 60 °C for 12 h, then DSC analyses were performed under nitrogen purging. The nonisothermal crystallization of the PLA/POE blends was monitored in the following procedure:

The samples were heated from the ambient temperature up to 200 °C at a heating rate of 20 °C/min then held for 5 min at 200 °C to remove their thermal history. Then, the samples were cooled to ambient temperature at different cooling rates of 5, 10, and 15 °C/min.

4. Results and Discussions

4.1. Morphological Observations

The SEM micrographs of various PLA/POE blends are shown in Figure 2 in order to monitor the effect of compatibilizer on the size reduction of rubber phase droplets. POE droplets removed by selective etching by xylene were displayed as dark holes, which were distributed in the PLA matrix. The results of the morphological evaluation in Figure 2 indicated a more uniform size and improved distribution of rubber phase droplets with the use of POEs based on PP. However, the results of image analysis for a minimum 200 dark holes indicated that there were no considerable changes in the size of the rubber phase with the introduction of EVA into the PLA/POE blends, whereas the incorporation of

EGMA into the prepared blends caused a drop in the POE droplets and a more uniform distribution, especially in the case of the PLA/POE blends containing Vistamaxx.

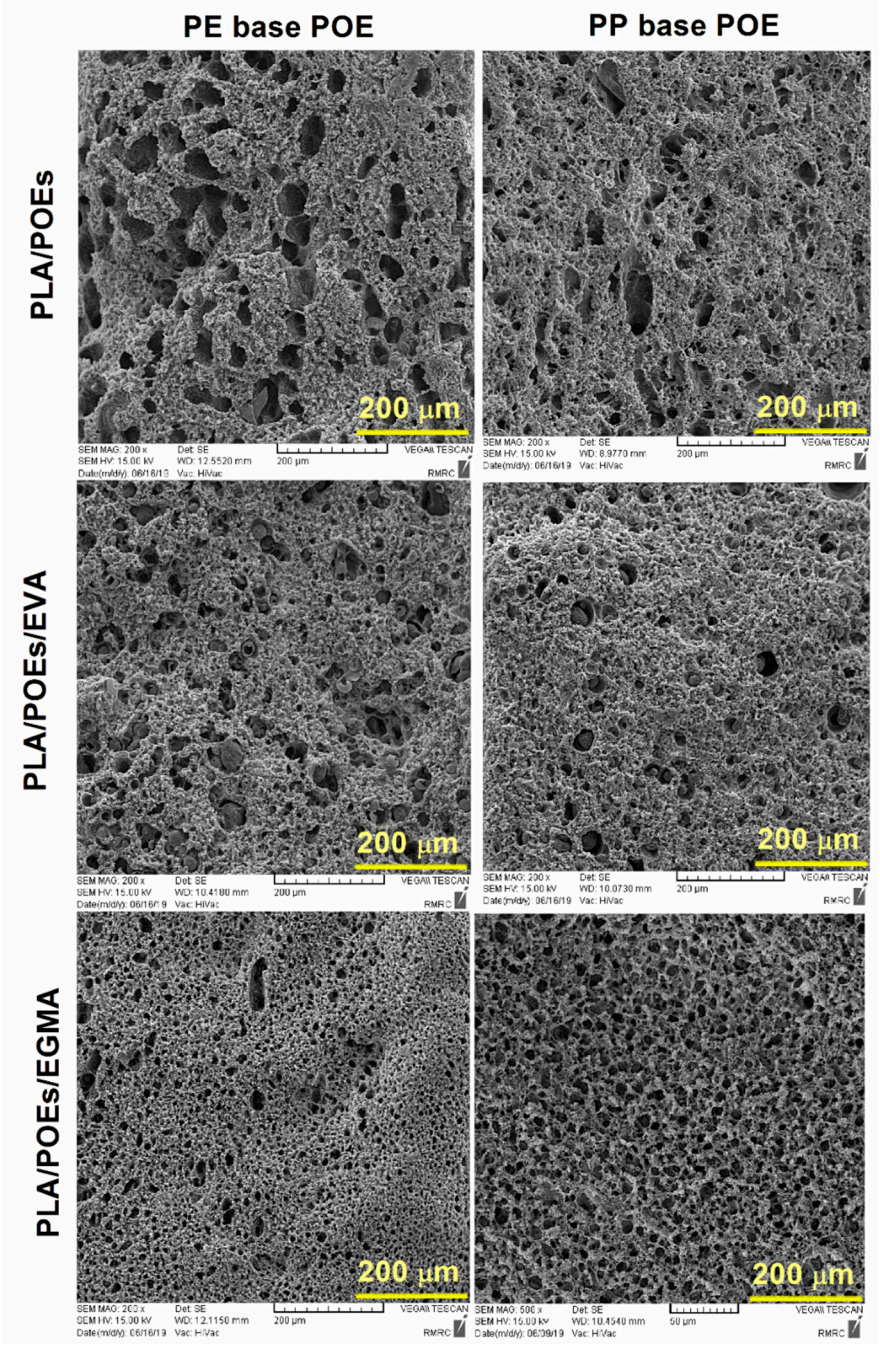


Figure 2. SEM photomicrographs of the prepared PLA/POE samples containing different compatibilizers.

Figure 3 shows the results of the statistical analysis of the rubber phase in the PLA/POE blends. Although the calculation of D_n could be useful, the distribution of particle size with weighing to the size of particles was carried out by calculating the D_v parameter. The bar chart in Figure 3 indicates that the samples containing EVA as the compatibilizer had a larger particle size up to 3 times of that of those compatibilized with EGMA.

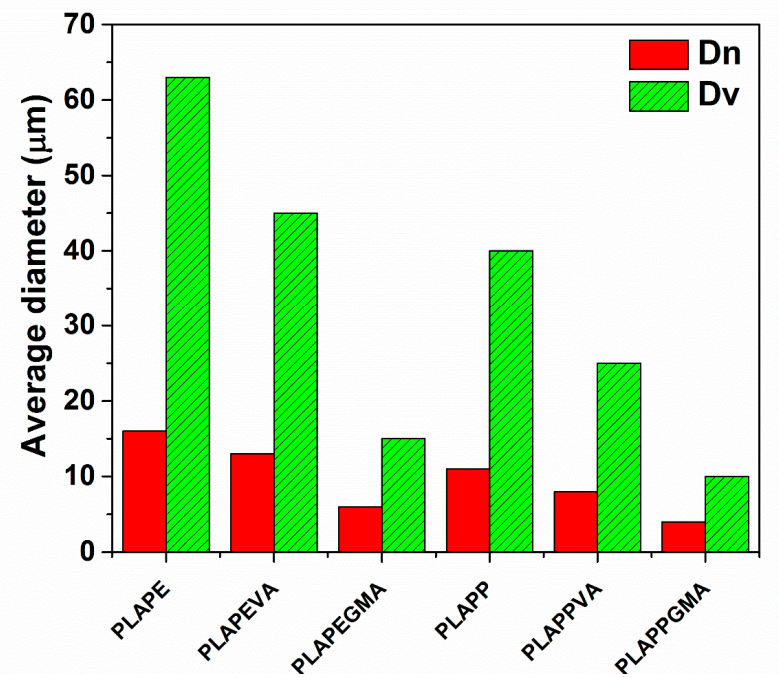


Figure 3. Variation of D_n and D_v of the dispersed phase in the PLA/POE blends.

4.2. Nonisothermal Crystallizations

Results of the nonisothermal crystallization at different cooling rates applied in DSC are provided in Figure 4. Table 2 gives the initial crystallization temperature, T_{c_0} (C), peak crystallization temperature, T_{c_p} (C), crystallization enthalpy, ΔH_c (J/g), crystallization temperature range, D (C), and crystallization time (s). As indicated in Table 2, with an increase of the cooling rate, the onset temperature decreased suggesting the retardation effect of POEs in the initial crystallization of PLA. Furthermore, the results presented in Table 2 revealed a fall in crystallization time with the introduction of the rubber phase, especially in the case of compatibilized PLA/POE blends.

The degree of crystallinity can be calculated based on melt crystallization using the following relationship [33]:

$$x = \frac{\Delta H}{\Delta H_m^0 \cdot w} \times 100, \tag{13}$$

where $\Delta H = \Delta H_c$ and ΔH_m^0 is the melting enthalpy of the 100% crystalline PLA equal to 93.0 J/g [34] and w is the weight percentage of PLA in the blend. As indicated in Table 2, the degree of crystallization decreased with addition of POEs due to an induced chain mobility in the PLA matrix [35]. As indicated in Table 2, the temperature range of crystallization reduced with the incorporation of the rubber phase into the PLA matrix, especially in the case of the PLA/POE blends containing the PE type rubber phase. However, this parameter increased with the presence of the compatibilizer in the PLA/POE blends.

According to the Figure 5 and the results presented in Table 2, it can be seen that the introduction of POEs into the PLA matrix, the enhancement in the cooling rate, and utilizing compatibilizers are each caused a decrease in T_{c_p}. This can be ascribed to the POEs that ibcrease the mobility of polymer chains, leading to a fall in the crystallinity of PLA [36]. It is obvious that the key parameter driving the crystallinity of a semi-crystalline polymer is the entrance of the polymer chains into the crystal cells, where this ability decreased with the introduction of a rubber phase with a higher chain mobility. However the reduction in T_{c_p} has become more obvious with the use of compatibilizer.

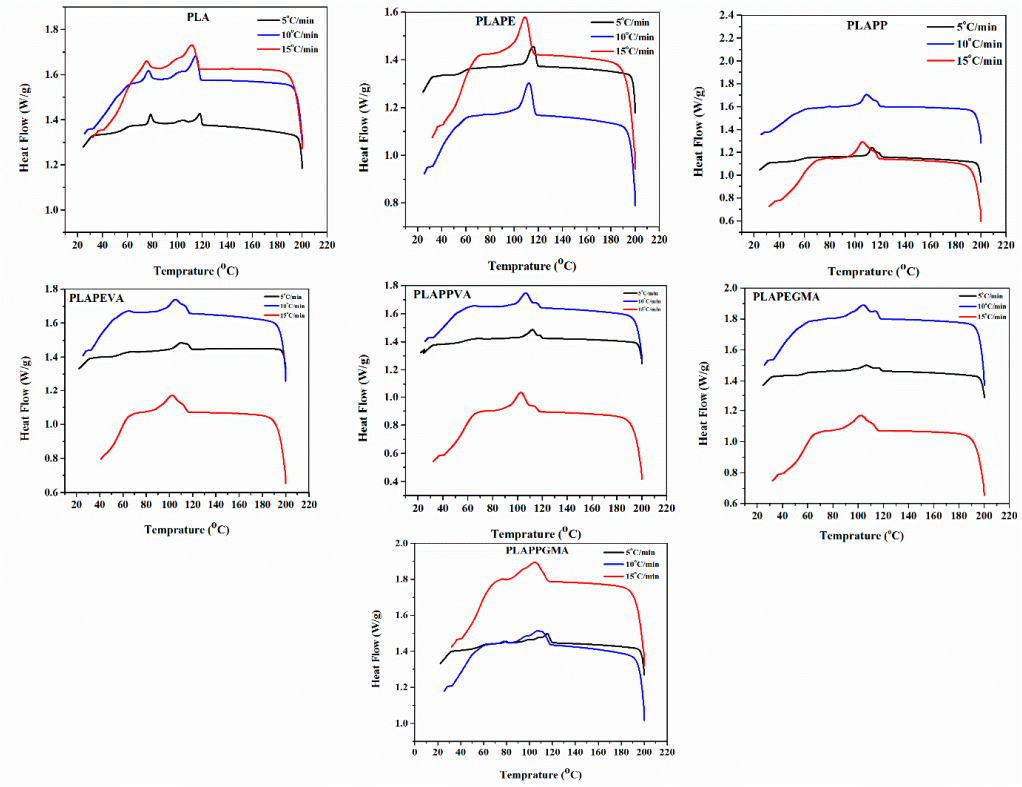


Figure 4. DSC thermograms of nonisothermal crystallization at different cooling rates for neat PLA and PLA/POE (80/20) with and without compatibilizer. Compatibilizers, EVA and EMA-GMA, were used at 4% phr.

Table 2. Crystallization parameters of various PLA/POE blends at various cooling rates derived from nonisothermal DSC measurements.

Samples	Cooling Rate (°C/min)	Initial Crystallization Temperature, T_{c_0} (°C)	Peak Temperature, T_{c_p} (°C)	Crystallization Enthalpy, ΔH_c (J/g)	Crystallization Temperature Range, D (°C)	Crystallization Time, (s)	Degree of Crystallization, (%)
PLA	5	122.29	118.10	9.50	48.41	9.68	10.22
	10	120.39	114.65	10.64	54.65	5.46	11.44
	15	118.87	111.66	12.52	55.84	3.72	13.46
PLAPE	5	122.19	115.94	6.62	20.08	4.02	8.89
	10	120.71	112.12	7.14	26.99	2.70	9.60
	15	119.59	109.01	7.06	32.73	2.18	9.48
PLAPEVA	5	121.62	110.02	5.37	23.83	4.77	7.22
	10	119.55	105.06	6.92	34.83	3.48	9.30
	15	117.59	102.00	6.61	39.21	2.61	8.89
PLAPEGMA	5	121.61	106.60	6.31	33.00	6.60	8.49
	10	119.86	104.07	8.89	37.66	3.77	11.95
	15	117.80	100.19	8.94	44.43	2.96	12.02
PLAPP	5	123.78	113.63	6.46	17.93	3.59	8.68
	10	122.87	109.31	7.03	31.66	3.17	9.45
	15	121.32	106.02	7.86	33.98	2.27	10.56
PLAPPVA	5	122.61	112.14	6.04	22.58	4.52	8.11
	10	120.55	106.59	7.07	32.16	3.22	9.50
	15	119.33	102.72	7.53	38.97	2.60	10.12
PLAPPGMA	5	121.02	115.52	7.60	33.25	6.65	10.21
	10	119.03	106.93	7.92	33.49	3.35	10.65
	15	118.08	104.60	7.70	37.97	2.53	10.35

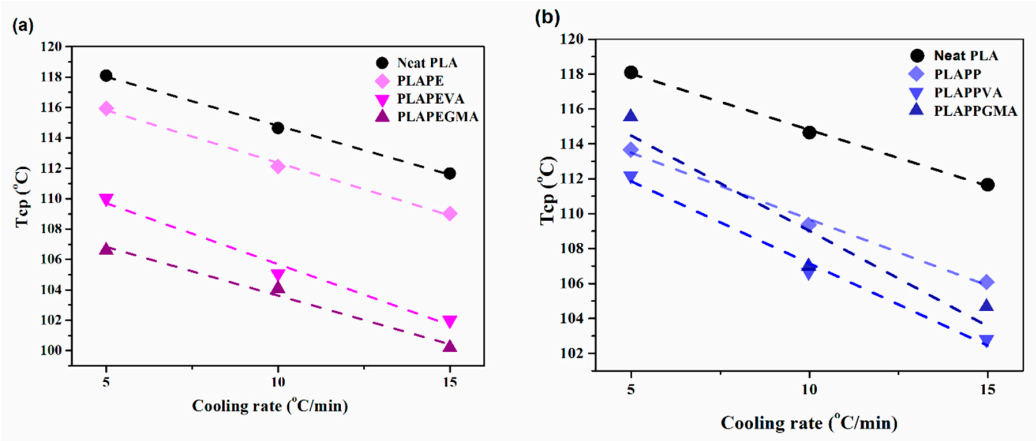


Figure 5. The effects of POEs, cooling rate, and compatibilizer on the peak crystallization temperature of the PLA matrix. (**a**) PLA blends containing PE base olefin elastomers. (**b**) PLA blends containing PP base olefin elastomers.

4.3. Crystallization Kinetics

The variation of $(1 - X_t)$ with time in the different cooling rates is provided in Figure 6. The resulting curves presented an upside down s-shaped form, showing the high dependency of $(1 - X_t)$ on the cooling rate for various PLA/POE blends. Table 3 shows the values of n, Z_C, and $t_{1/2}$, where the Avrami parameters, n, and Z_C , are calculated from the curves in Figure 7. The parameter n can give information about the nature of nucleation and growth processes. Moreover, site saturation may lead to n values of 1, 2, or 3 for the surface, edge, and point sites, respectively [37].

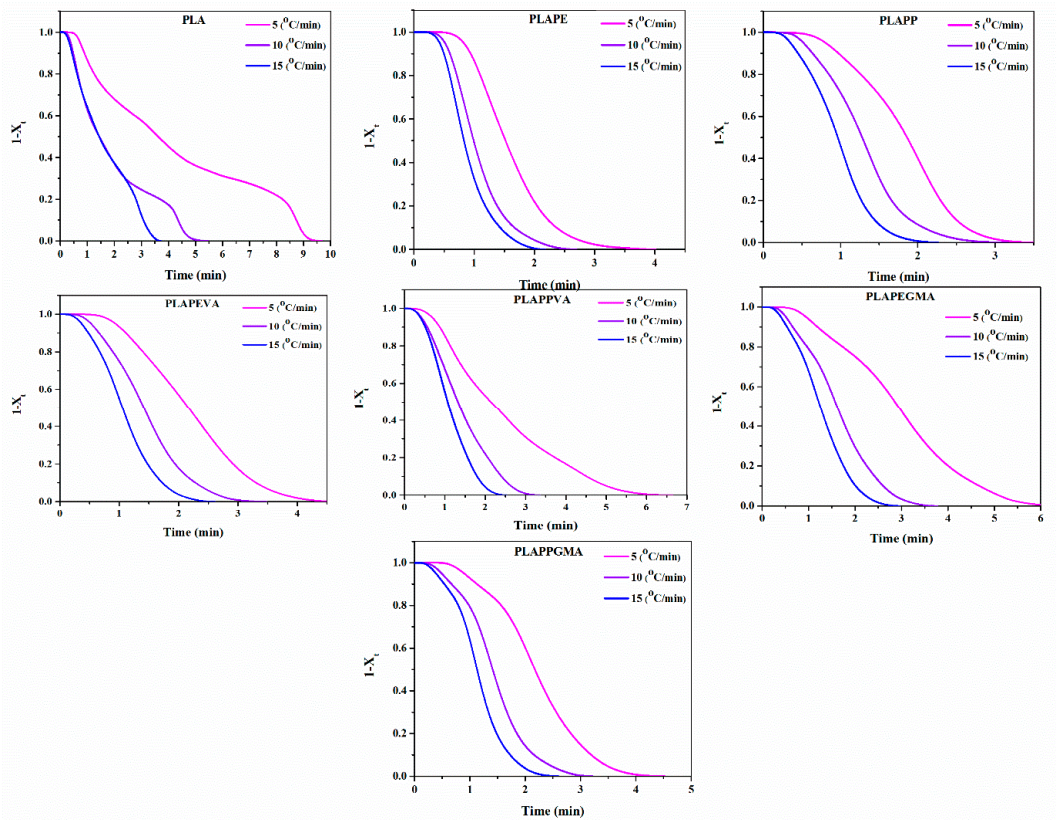


Figure 6. Variation of $(1 - X_t)$ as a function of time for the neat PLA and PLA/POE (80/20) with and without compatibilizer. Compatibilizers, EVA and EMA-GMA, were used at 4% phr.

Table 3. Crystallization kinetic parameters at various cooling rates for the various PLA/POEs based on the Avrami model.

Cooling Rate (°C/min)	Samples	n	Z_C	$t_{1/2}$ (min)
5		1.20	0.68	3.61
10	**PLA**	1.27	0.91	2.04
15		1.41	0.94	1.39
5		3.28	0.69	1.52
10	**PLAPE**	2.98	0.95	1.02
15		2.89	1.00	0.83
5		3.22	0.64	1.86
10	**PLAPP**	2.84	0.90	1.64
15		2.66	0.99	1.18
5		2.77	0.61	2.17
10	**PLAPEVA**	2.52	0.88	1.58
15		2.45	0.97	1.19
5		3.09	0.58	2.17
10	**PLAPPVA**	2.77	0.88	1.55
15		2.79	0.95	1.25
5		2.29	0.58	2.93
10	**PLAPEGMA**	2.28	0.87	1.67
15		2.36	0.94	1.31
5		1.77	0.70	2.14
10	**PLAPPGMA**	2.08	0.91	1.08
15		2.43	0.96	0.81

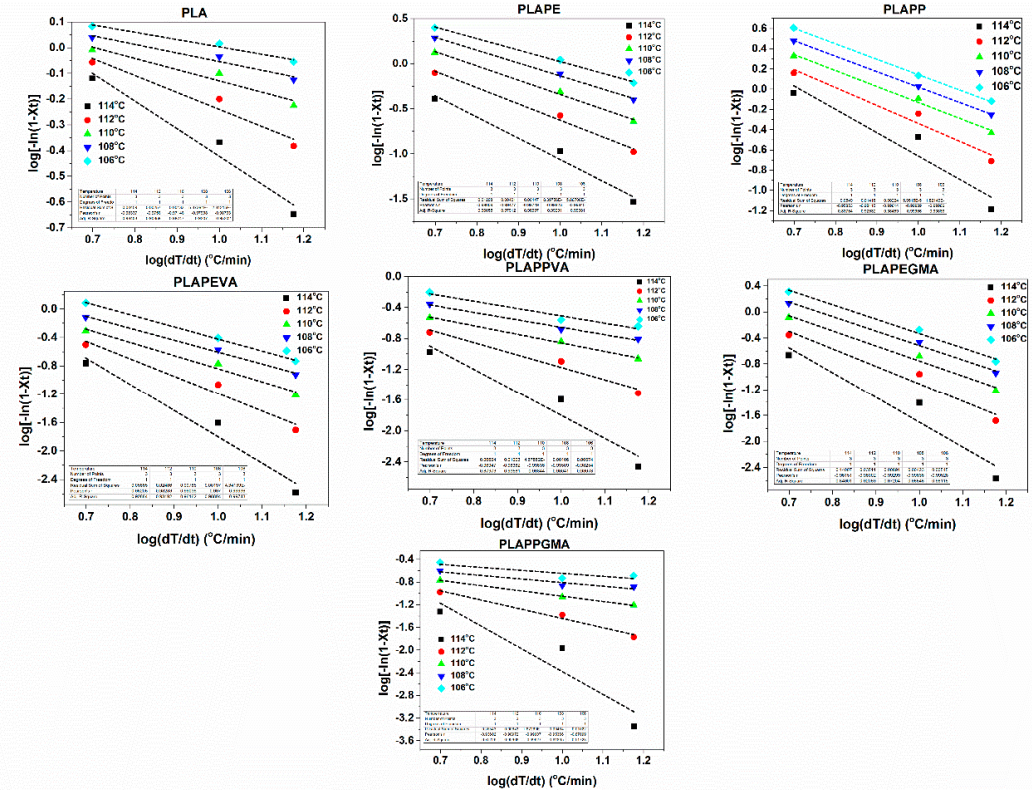


Figure 7. Variation of $\log[-\ln(1-X_t)]$ as a function of $\log\left(\frac{dT}{dt}\right)$ for the neat PLA and PLA/POE (80/20) with and without compatibilizer. Compatibilizers, EVA and EMA-GMA, were used at 4% phr.

The parameter n for the neat PLA changed between 1.18–1.41, which indicates that the thermal process did not have any significant effect on this factor. For the neat PLA, the values of n indicated a simultaneous and circular layer growth of spherulites, which converted to sporadic growth with

the addition of POEs. As indicated in Table 3, the values of n increased up to 3 for uncompatibilized PLA/POE blends, whereas the parameter n was about 2–3 for compatibilized PLA/POE blends due to the induced chain mobility in PLA, which led to a decreased crystallinity. The value of n reduced with an increase in the cooling rate for all compatibilized and non-compatibilized PLA/POE blends, except in the PLAPPGMA sample code, which has a growing trend, indicating the variation of crystallization kinetics with higher cooling rates [36,38]. The results suggest a more complicated crystallization kinetics in PLA/POE blends containing EGMA compatibilizers. The results of the nonisothermal crystallization rate, Z_C, as displayed in Table 3, show an increase with higher cooling rates in various PLA/POE blends. The parameter Z_C shows the rate of growing crystals, which had an inverse relation with compatibility. However, in the absence of compatibilizers, the surface of POE particles had a high energy, which would be good points for nucleation due to the provision of the activation energy needed for this process. As can be seen in Table 3, there is an inverse relationship between $t_{1/2}$ and cooling rate. This value has a slight reduction in PLA/POE blends compared to neat PLA.

The relationship between $\log[-\ln(1-X_t)]$ and $\log\left(\frac{dT}{dt}\right)$ in Figure 7 is linear, which indicates that the Ozawa model for seeking the nonisothermal crystallization behavior of PLA/POE blends is acceptable. Various parameters of the Ozawa model are presented in Table 4. Accordingly, m decreased with temperature. The Ozawa exponent, m, has a relation with the dimension of nucleation growth, where the values of 0, 1, and 2 are referred to as one, two, and three dimensional growths [7].

Table 4. Crystallization kinetic parameters at various cooling rates for various PLA/POE blends based on the Ozawa equation.

Samples	T (°C)	m	K (min^{-1})	Samples	T (°C)	m	K (min^{-1})
	118	0.01	0.10		116	0.23	0.11
	116	0.03	0.22		115	0.05	0.22
	113	0.08	0.36		113	0.21	0.35
	108	0.07	0.51		112	0.06	0.51
PLA	104	0.00	0.69	**PLAPEVA**	111	0.08	0.69
	100	0.01	0.92		110	0.02	0.92
	91	0.00	1.20		108	0.09	1.20
	81	0.06	1.61		107	0.10	1.61
	79	0.04	2.30		105	0.06	2.30
	117	0.92	0.10		117	0.06	0.11
	117	0.09	0.22		115	0.04	0.22
	116	0.18	0.36		114	0.02	0.36
	115	0.05	0.51		113	0.29	0.51
PLAPE	115	0.01	0.69	**PLAPPEVA**	112	0.07	0.69
	114	0.13	0.91		111	0.20	0.92
	113	0.19	1.20		110	0.17	1.21
	112	0.06	1.60		108	0.08	1.61
	110	0.00	2.30		107	0.01	2.30
	119	0.26	0.11		116	0.33	0.10
	117	0.18	0.22		113	0.08	0.22
	116	0.14	0.35		110	0.15	0.36
	115	0.18	0.51		108	0.09	0.51
PLAPP	114	0.12	0.69	**PLAPEGMA**	107	0.00	0.69
	114	0.21	0.92		105	0.00	0.91
	113	0.18	1.21		104	0.17	1.20
	112	0.09	1.60		102	0.03	1.61
	111	0.02	2.30		98	0.08	2.30
	117	0.17	0.11		117	0.17	0.11
	115	0.22	0.22		115	0.22	0.22
	114	0.08	0.36		114	0.08	0.36
	112	0.01	0.51		112	0.01	0.51
PLAPPGMA	110	0.03	0.69	**PLAPPGMA**	110	0.03	0.69
	108	0.09	0.91		108	0.09	0.91
	106	0.03	1.20		106	0.03	1.20
	102	0.12	1.61		102	0.12	1.61
	98	0.09	2.30		98	0.09	2.30

The results of the crystallization kinetics of PLA/POEs using the Ozawa model suggest that the values of parameter m remain close to zero at most temperatures for various PLA/POE blends, which indicates that the crystallization of PLA remains in one dimensional growth.

According to Figure 8, it can be seen that the crystallization of the PLA/POE blends were completed in less time rather than with neat PLA. This means that the crystallization duration of the PLA/POE blends decreased in comparison with the neat PLA, whereas a decrease in the cooling rate led to a complete crystallization of PLA in a shorter time period. Figure 8 reveals that the incorporation of POEs into the PLA matrix caused rapid crystallization, despite a general reduction in the crystallinity.

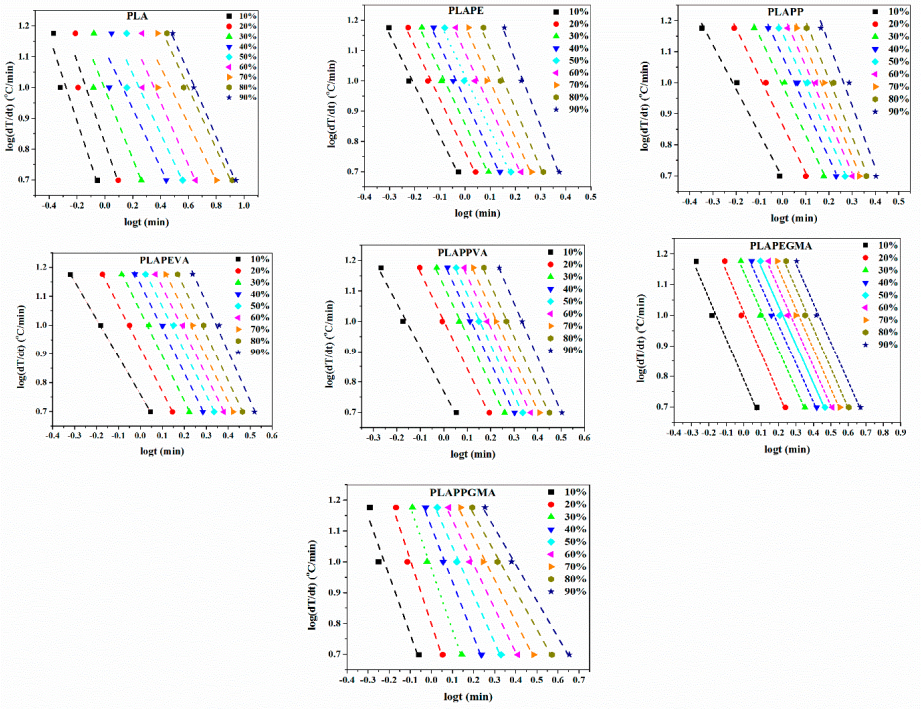


Figure 8. Plots of the cooling rates as a function of cooling time for the neat PLA and PLA/POE (80/20) with and without compatibilizer. Compatibilizers, EVA and EMA-GMA, were used at 4% phr.

Parameters of the Mo model are provided in Table 5. As can be seen, both parameters of the MO model, a and $\log F(T)$, increased with cooling rates for various PLA/POE blends, which implies a higher rate of the crystallization process. However, the trends in a and $\log F(T)$ for various PLA/POE blends showed that the introduction of POEs into the PLA matrix led to a decrease in the crystallization rate of PLA, especially in the case of PP based POEs. The results in Table 5 indicate a lower value for a and $\log F(T)$ with the addition of compatibilizer, especially for PLA/POEs containing the PP base POEs and EGMA as a compatibilizer. Consequently, the study of the crystallization kinetics of PLA/POE blends by using the Mo model suggested a lower crystallization rate with the incorporation of POEs and compatibilizer at a certain cooling rate, compared to neat PLA.

Table 5. Crystallization kinetic parameters at various cooling rates for the PLA/POE blends based on the Mo model.

Cooling Rate (°C/min)	Samples	a	log$F(T)$	Samples	a	log$F(T)$	Samples	a	log$F(T)$
5		2.19	0.69		1.43	0.69		1.38	0.62
10	**PLA**	2.39	0.99	**PLAPEVA**	1.55	0.87	**PLAPPGMA**	1.33	0.82
15		2.24	1.21		1.60	0.99		1.13	1.00
5		1.33	0.79		1.45	0.54			
10	**PLAPE**	1.34	1.01	**PLAPPVA**	1.54	0.67			
15		1.28	1.14		1.57	0.79			
5		1.31	0.76		1.69	0.65			
10	**PLAPP**	1.50	0.92	**PLAPEGMA**	1.74	0.77			
15		1.56	1.05		1.77	0.86			

Figure 9 depicts the values of $\ln\left(\frac{\frac{dT}{dt}}{T_{cp}^2}\right)$ as a function of $\frac{1000}{Tc_p}$, where the slope of each resulting straight line gives the activation energy needed for the crystallization of various PLA/POE blends The values of crystallization activation energy for each of the prepared samples are plotted in Figure 10. It is obvious that the activation energy for the crystallization of PLA decreased with the incorporation of POEs, especially with the PP based olefin elastomer. In addition, the use of compatibilizer led to more reduction in the activation energy, especially in the case of PLA/POEs containing an EGMA compatibilizer. The results recommend a lower activation energy for the crystallization of a PLA matrix in samples with more reduced rubber phase droplets, in accordance with the results of the SEM photomicrographs.

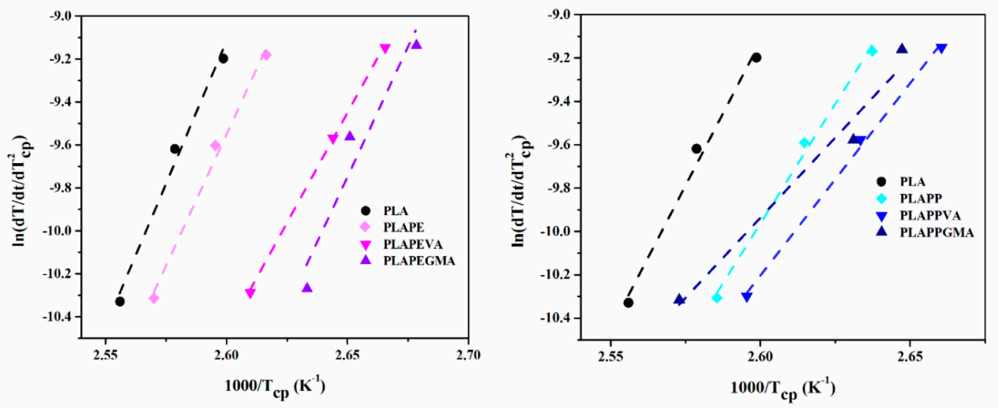


Figure 9. Plots for evaluating the crystallization activation energy for the comparison between different compositions of compatibilized and non compatibilized PLA/POE blends with neat PLA for each grade of POE based on the Kissinger model.

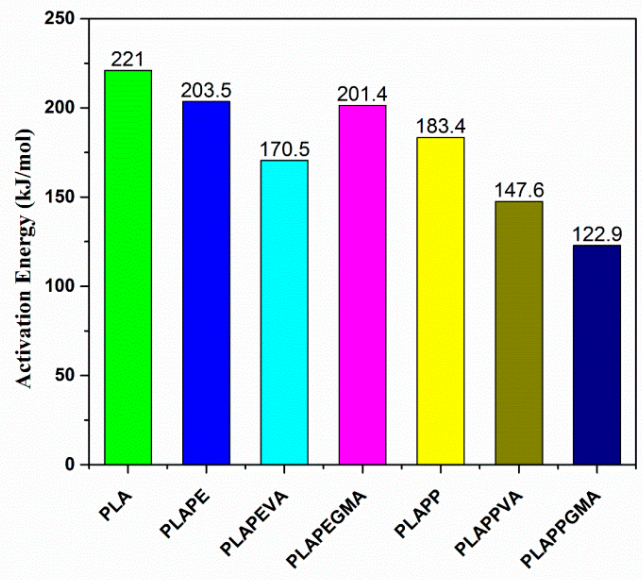


Figure 10. Nonisothermal crystallization activation energy for various PLA/POEs based on the Kissinger model.

5. Conclusions

Various PLA/POE blends were prepared via melt mixing process and the effects of POE type, and compatibilizer type were monitored using crystallization kinetic parameters of the PLA matrix. Assessments made on morphology indicated that the presence of EGMA as a compatibilizer had an effective role in the distribution of the POE phase in the PLA matrix, especially in blends containing

a PP base POE. Crystallization kinetics of the PLA matrix under the effect of various POEs and compatibilizer were surveyed using the Avrami, Ozawa, Mo, and Kissinger models. The resulting DSC diagrams indicated that the initial crystallization temperature of the PLA matrix shifted to a lower temperature with the introduction of various POEs into the PLA matrix, and the addition of a compatibilizer helped with this trend. The investigation of the crystallization kinetics of PLA/POEs through the Avrami model indicated a decreased crystallinity with the introduction of POEs into the PLA matrix, especially in the case of a PP base olefin elastomer. Crystallization kinetics analysis of PLA/POEs using Ozawa model suggested that the crystallization of PLA remains one dimensionally growthed with varying the POE and compatibilizer types. The investigation of the crystallization kinetics of the PLA/POE blends using the Mo model suggested a lower crystallization rate with the incorporation of POEs and compatibilizer at a certain cooling rate. Kissinger model revealed that the activation energy for the crystallization of PLA decreased with the incorporation of POEs, especially in the case of the PP based olefin elastomer. Likewise, the use of compatibilizer led to a more reduction in the activation energy, especially in the case of PLA/POEs containing the EGMA compatibilizer.

Author Contributions: Conceptualization, M.R.S.; Methodology, S.M.R.P. and M.R.S.; Software, S.M.R.P.; Validation, A.F., M.M.K., and M.R.S.; Formal analysis, A.K. and H.V.; Investigation, V.B. and G.N.; Data curation, S.M.R.P.; Writing—original draft preparation, A.K.; Writing—review and editing, S.M.R.P.; Visualization, S.M.R.P.; Supervision, S.M.R.P. and M.R.S. All authors have read and agreed to the published version of the manuscript.

Funding: This research received no external funding.

Acknowledgments: The authors would like to acknowledge the Center of Excellence in Electrochemistry, School of Chemistry, College of Science, University of Tehran for providing the authors with laboratory equipment.

Conflicts of Interest: The authors declare no conflict of interest.

References

1. Yang, S.-L.; Wu, Z.; Yang, W.; Yang, M.-B. Thermal and mechanical properties of chemical crosslinked polylactide (PLA). *Polym. Test.* **2008**, *27*, 957–963. [CrossRef]
2. Farah, S.; Anderson, D.G.; Langer, R. Physical and mechanical properties of PLA, and their functions in widespread applications—A comprehensive review. *Adv. Drug Deliv. Rev.* **2016**, *107*, 367–392. [CrossRef] [PubMed]
3. Myers, M.; Felty, E. Structural characterizations of vitreous inorganic polymers by thermal studies. *Mater. Res. Bull.* **1967**, *2*, 535–546. [CrossRef]
4. Perego, G.; Cella, G.D.; Bastioli, C. Effect of molecular weight and crystallinity on poly (lactic acid) mechanical properties. *J. Appl. Polym. Sci.* **1996**, *59*, 37–43. [CrossRef]
5. Kong, Y.; Hay, J. The measurement of the crystallinity of polymers by DSC. *Polymer* **2002**, *43*, 3873–3878. [CrossRef]
6. Lu, X.; Hay, J. Isothermal crystallization kinetics and melting behaviour of poly(ethylene terephthalate). *Polymer* **2001**, *42*, 9423–9431. [CrossRef]
7. Ozawa, T. Kinetics of non-isothermal crystallization. *Polymer* **1971**, *12*, 150–158. [CrossRef]
8. Chapleau, N.; Huneault, M.A.; Li, H. Biaxial Orientation of Polylactide/Thermoplastic Starch Blends. *Int. Polym. Process.* **2007**, *22*, 402–409. [CrossRef]
9. Lee, R.E.; Guo, Y.; Tamber, H.; Planeta, M.; Leung, S.N.S. Thermoforming of polylactic acid foam sheets: Crystallization behaviors and thermal stability. *Ind. Eng. Chem. Res.* **2016**, *55*, 560–567. [CrossRef]
10. Serra, T.; Planell, J.A.; Navarro, M. High-resolution PLA-based composite scaffolds via 3-D printing technology. *Acta Biomater.* **2013**, *9*, 5521–5530. [CrossRef]
11. Harris, A.M.; Lee, E.C. Improving mechanical performance of injection molded PLA by controlling crystallinity. *J. Appl. Polym. Sci.* **2007**, *107*, 2246–2255. [CrossRef]
12. Saeidlou, S.; Huneault, M.A.; Li, H.; Park, C.B. Poly(lactic acid) crystallization. *Prog. Polym. Sci.* **2012**, *37*, 1657–1677. [CrossRef]
13. Kulinski, B.; Piorkowska, E. Crystallization, structure and properties of plasticized poly(l-lactide). *Polymer* **2005**, *46*, 10290–10300. [CrossRef]

14. Yokohara, T.; Yamaguchi, M. Structure and properties for biomass-based polyester blends of PLA and PBS. *Eur. Polym. J.* **2008**, *44*, 677–685. [CrossRef]
15. Pantani, R.; De Santis, F.; Sorrentino, A.; De Maio, F.; Titomanlio, G. Crystallization kinetics of virgin and processed poly (lactic acid). *Polym. Degrad. Stab.* **2010**, *95*, 1148–1159. [CrossRef]
16. Jun, C.L. Reactive Blending of Biodegradable Polymers: PLA and Starch. *J. Polym. Environ.* **2000**, *8*, 33–37. [CrossRef]
17. Liu, H.; Song, W.; Chen, F.; Guo, L.; Zhang, J. Interaction of microstructure and interfacial adhesion on impact performance of polylactide (PLA) ternary blends. *Macromolecules* **2011**, *44*, 1513–1522. [CrossRef]
18. Esmizadeh, E.; Sadeghi, T.; Vahidifar, A.; Naderi, G.; Ghoreishy, M.H.R.; Paran, S.M.R. Nano Graphene-Reinforced Bio-nanocomposites Based on NR/PLA: The Morphological, Thermal and Rheological Perspective. *J. Polym. Environ.* **2019**, *27*, 1529–1541. [CrossRef]
19. Zhang, C.; Wang, W.; Huang, Y.; Pan, Y.; Jiang, L.; Dan, Y.; Luo, Y.; Peng, Z. Thermal, mechanical and rheological properties of polylactide toughened by expoxidized natural rubber. *Mater. Des.* **2013**, *45*, 198–205. [CrossRef]
20. Balakrishnan, H.; Hassan, A.; Wahit, M.U. Mechanical, thermal, and morphological properties of polylactic acid/linear low density polyethylene blends. *J. Elastomers Plast.* **2010**, *42*, 223–239. [CrossRef]
21. Xu, Y.; Delgado, P.; Todd, A.D.; Loi, J.; Saba, S.A.; McEneany, R.J.; Tower, T.; Topolkaraev, V.; Macosko, C.W.; Hillmyer, M. Lightweight micro-cellular plastics from polylactide/polyolefin hybrids. *Polymer* **2016**, *102*, 73–83. [CrossRef]
22. Heshmati, V.; Zolali, A.M.; Favis, B.D. Morphology development in poly (lactic acid)/polyamide11 biobased blends: Chain mobility and interfacial interactions. *Polymer* **2017**, *120*, 197–208. [CrossRef]
23. Imre, B.; Bedő, D.; Domján, A.; Schön, P.; Vancso, G.J.; Pukánszky, B. Structure, properties and interfacial interactions in poly (lactic acid)/polyurethane blends prepared by reactive processing. *Eur. Polym. J.* **2013**, *49*, 3104–3113. [CrossRef]
24. Wen, S.; Yan, L.; Gong, C.; Zheng, G.; Zhou, Y. Preparation and performance of the polylactic acid/polyolefin-elastomer/thermoplastic starch composite materials. *Chin. J. Colloid Polym.* **2011**, *29*, 81–83.
25. Wu, M.; Wu, Z.; Wang, K.; Zhang, Q.; Fu, Q. Simultaneous the thermodynamics favorable compatibility and morphology to achieve excellent comprehensive mechanics in PLA/OBC blend. *Polymer* **2014**, *55*, 6409–6417. [CrossRef]
26. Jiang, J.; Su, L.; Zhang, K.; Wu, G. Rubber-toughened PLA blends with low thermal expansion. *J. Appl. Polym. Sci.* **2012**, *128*, 3993–4000. [CrossRef]
27. Wu, M.; Wang, K.; Zhang, Q.; Fu, Q. Manipulation of multiphase morphology in the reactive blending system OBC/PLA/EGMA. *RSC Adv.* **2015**, *5*, 96353–96359. [CrossRef]
28. Paran, S.M.R.; Vahabi, H.; Ducos, F.; Formela, K.; Zarrintaj, P.; Laachachi, A.; Saeb, M.R. Crystallization kinetics study of dynamically vulcanized PA6/NBR/HNTs nanocomposites by nonisothermal differential scanning calorimetry. *J. Appl. Polym. Sci.* **2018**, *135*, 46488. [CrossRef]
29. Balazs, A. Crystallization Kinetics of Commercial PLA Filament. *Commun.-Sci. Lett. Univ. Zilina* **2017**, *19*, 15–19.
30. Bianchi, O.; Oliveira, R.; Fiorio, R.; Martins, J.D.N.; Zattera, A.; Canto, L. Assessment of Avrami, Ozawa and Avrami–Ozawa equations for determination of EVA crosslinking kinetics from DSC measurements. *Polym. Test.* **2008**, *27*, 722–729. [CrossRef]
31. Zhang, Z.; Chen, J.; Liu, H.; Xiao, C. Applicability of Kissinger model in nonisothermal crystallization assessed using a computer simulation method. *J. Therm. Anal. Calorim.* **2014**, *117*, 783–787. [CrossRef]
32. Rastin, H.; Jafari, S.H.; Saeb, M.R.; Khonakdar, H.A.; Wagenknecht, U.; Heinrich, G. Mechanicalrheological, and thermal behavior assessments in HDPE/PA-6/EVOH ternary blends with variable morphology. *J. Polym. Res.* **2014**, *21*, 352. [CrossRef]
33. Battegazzore, D. Crystallization kinetics of poly(lactic acid)-talc composites. *Express Polym. Lett.* **2011**, *5*, 849–858. [CrossRef]
34. Garlotta, D. A Literature Review of Poly(Lactic Acid). *J. Polym. Environ.* **2001**, *9*, 63–84. [CrossRef]

35. Rosli, N.A.; Ahmad, I.; Anuar, F.H.; Abdullah, I. Mechanical and thermal properties of natural rubber-modified poly(lactic acid) compatibilized with telechelic liquid natural rubber. *Polym. Test.* **2016**, *54*, 196–202. [CrossRef]
36. Hay, J.N. Application of the modified avrami equations to polymer crystallisation kinetics. *Br. Polym. J.* **1971**, *3*, 74–82. [CrossRef]
37. Cahn, J.W. Transformation kinetics during continuous cooling. *Acta Met.* **1956**, *4*, 572–575. [CrossRef]
38. Sharples, A. Overall kinetics of crystallization. In *Introduction to Polymer Crystallization*; St. Martin's Press: New York, NY, USA, 1966; pp. 44–59.



© 2020 by the authors. Licensee MDPI, Basel, Switzerland. This article is an open access article distributed under the terms and conditions of the Creative Commons Attribution (CC BY) license (http://creativecommons.org/licenses/by/4.0/).